Preprints of the 21st IFAC World Congress (Virtual)
Berlin, Germany, July 12-17, 2020

LSTM-based IMC approach applied in Wastewater Treatment Plants: performance and stability analysis

I. Pisa [*,**], **A. Morell** [*], **J.L. Vicario** [*], **R. Vilanova** [**]

[*] *Wireless Information Networking (WIN) Group*
[**] *Advanced Systems for Automation and Control (ASAC) Group*
Universitat Autònoma de Barcelona, Bellaterra, Spain

Abstract: Wastewater treatment plants are industries where the reduction of residual water pollutant concentrations is performed. These kind of industries are characterised by applying highly complex and nonlinear biochemical and biological processes. Thus, some of the concentrations involved in these processes have to be controlled to assure that they are maintained at a given set-point. For that reason, different control strategies such as Proportional Integral (PI) controllers, Model Predictive Controllers (MPC), Fuzzy Logic or Internal Model Controllers (IMC) have been applied during the last years. However, the appearance of Artificial Neural Networks (ANNs) is changing this scenario. They have been adopted to predict certain WWTP parameters and then feed conventional controllers or even to implement some of them. Here, an IMC approach implemented uniquely with Long Short-Term Memory (LSTM) cells to model the direct and inverse models of the process under control is proposed. Furthermore, its stability conditions are computed adopting a data-based test since no mathematical expressions of the different models are considered. Results show that this approach is stable in the frequency region where it is operating. Besides, control performance shows that this IMC is able to significantly improve the Benchmark Simulation Model No.1 default PI control strategy.

Keywords: Artificial Neural Networks, Data-based control, Internal Model Control, Robust Control, Wastewater Treatment processes.

1. INTRODUCTION

Nowadays, nearly all the industrial processes are being controlled to assure they are yielding coherent values instead of incoherent ones. In that sense, Wastewater Treatment Plants (WWTP) are one of the industries where control strategies are considered in most of the processes they perform. The main objective of WWTPs is to treat urban residual waters to reduce the amount of pollutants and then spill the clean water into its natural cycle. To achieve this reduction, WWTPs apply highly complex and non-linear biological and biochemical processes to transform the pollutant products into harmless ones. However, these processes not always remove the pollutant products completely. For that reason, regulations have been applied in the form of limits specifying the maximum allowed concentrations of pollutants. One clear example of them is the European Directive 91/271 (Directive, EUW (1991)).

The biological and biochemical processes involved in the pollutant reduction require certain parameters set at a constant level depending on the pollutant concentrations. For that reason, different control strategies have been considered accordingly to the type of WWTP. Since there are a lot of WWTP architectures, the International Water Association developed a WWTP framework simulating the real behaviour of a general purpose plant, the Benchmark Simulation Model No.1 (BSM1), whose main aim is to offer generalisation, easy comparison and replicability of results. Thus, any control strategy to be applied in WWTPs can be tested previously in BSM1 (Copp (2002)).

The great majority of control strategies applied in WWTP industries are devoted to managing certain concentrations taking into account measurements from the different reactor tanks. This is the case of the BSM1 default control strategy (Alex et al. (2008)). It tries to maintain the pollutant concentrations at a given point in order to accomplish the regulations that apply, however, some violation of pollutant concentration limits are still produced (Alex et al. (2008)). For that reason, different and more complex control strategies such as Model Predictive Controllers (MPCs), Fuzzy Logic, and Internal Model Controllers (IMCs) have been considered to improve the WWTPs control performance. For instance, in Shen et al. (2008), two non-linear MPC approaches have been adopted to maintain the effluent quality below regulation limits. Another approach corresponds to a supervised committee Fuzzy Logic model which has been applied in Nadiri et al. (2018) to predict the Chemical Oxygen Demand (COD), the Biochemical Oxygen Demand (BOD) and the Total Sus-

⋆ This research is supported by the Catalan Government under Projects 2017 SGR 1202 and 2017 SGR 1670, by La Secretaria dUniversitats i Recerca del Departament dEmpresa i Coneixement de la Generalitat de Catalunya i del Fons Social Europeu under FI grant and also by the Spanish Government under Projects TEC2017-84321-C4-4-R and DPI2016-77271-R co-funded with the European Regional Development Funds of the European Union.

pended Solids (TSS) concentrations. Finally, in Vilanova et al. (2018), an event-based IMC has been considered to improve the BSM1 default control strategy.

The evolution of industry towards the Industry 4.0 paradigm as well as the incursion of Artificial Neural Networks (ANNs) are changing the way of controlling industrial processes (Sarvari et al. (2018)). In this case, the adoption of ANNs in control strategies vary depending on their purpose. For instance, ANNs are considered in some cases to predict WWTP effluent concentrations and then feed Fuzzy Logic (Qiao et al. (2018)) or MPC solutions (Sadeghassadi et al. (2018)). In other cases, the ANNs determine which control strategy has to be adopted and when it has to be activated (Pisa et al. (2019b)). They have also been considered to implement the control actuation. For instance, some IMCs consider ANNs to get the direct and inverse relationship between the actuation variables and the controlled ones. Doing so they are able to decouple the complexity of the process under control from the control itself (Pisa et al. (2019a)).

In this work, a data-based IMC strategy has been considered due to its simplicity, easy implementation and good control performance (Vilanova et al. (2018)). This new IMC approach, which adopts ANNs to implement the direct and inverse models of the process under control, will be in charge of controlling the dissolved oxygen ($S_{O,5}$) of the last WWTP aerated tank. The same approach was considered in Pisa et al. (2019a), however, the stability of the Multilayer Perceptron (MLP)-based IMC was not computed. Here, the MLP nets will be substituted by Long Short-Term Memory (LSTM) cells, which are able to generate a prediction model considering the time-correlation between measurements. Furthermore, the stability of this new IMC approach will be computed here to determine the suitability of the controller and its frequency behaviour.

The structure of this work is as follows. The problem conducted here and the proposed ANN-based solution are presented in Sections 2 and 3. Then, the study of its stability as well as the results obtained after evaluating the proposed solution are shown in Sections 4 and 5. The last section concludes the paper.

2. PROBLEM DEFINITION

BSM1 architecture considers five reactor tanks where the biological and biochemical processes described by the Activated Sludge Model No.1 (ASM1) are implemented (Henze et al. (1987)). Its default control strategies are focused on tracking the nitrate-nitrogen ($S_{NO,2}$) and dissolved oxygen ($S_{O,5}$) set-points (1 mg/L and 2 mg/L, respectively) by means of PI controllers (see Fig. 1). Here, we are going to focus on the second control loop, the one in charge of the $S_{O,5}$ set-point. This PI controller regulates the $S_{O,5}$ concentration to get 2 mg/L by means of modifying the oxygen transfer coefficient of the fifth reactor tank ($K_{La,5}$). However, it is observed that certain violations of effluent pollutant concentrations are not avoided (Alex et al. (2008)). For that reason, a new IMC control strategy improving the default control will be implemented. It is characterised by explicitly introducing the process under control ($P(z)$) in the control loop (see Fig. 2). Besides, it implements two mathematical models, the direct ($P_{dir}(z)$)

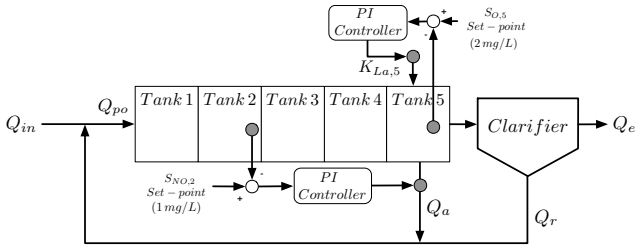

Fig. 1. BSM1 default control. Q_{in}, Q_{po}, Q_a, Q_r and Q_e are the influent, the primary overflow, the internal and external recirculation and the effluent flow rates, respectively.

and its inverse ($P_{inv}(z)$), which model the direct and inverse relationships between the actuation ($u[n]$) and the controlled ($y[n]$) variables. The signal $\tilde{y}[n]$, which acts as an input of the inverse model P_{inv}, corresponds to the reference signal ($r[n]$) modified with the mismatch between the real process $P(z)$ and the direct model $P_{dir}(z)$. Therefore, the higher the accuracy of the models, the better the IMC performance. However, the process under control is usually highly-complex and non-linear. Thus, it has to be linearised to determine $P_{dir}(z)$ and $P_{inv}(z)$ and therefore, the accuracy of these models can be compromised.

As previously stated, the increasing interest on ANNs is motivating their adoption in the control and automation processes (Sarvari et al. (2018)) due to their ability in modelling non-linear processes such as the ones present in WWTP facilities (Da Silva et al., 2017, Chapter 1). For instance, in Pisa et al. (2019a) two MLPs were considered to implement the $P_{dir}(z)$ and $P_{inv}(z)$ models required by the IMCs which substitute the PI controlling the $S_{O,5}$ set-point. However, these networks are not able to take into account the time-correlation between measurements since they do not implement any memory cell. For that reason, LSTM cells will be considered to implement the IMC due to their suitability dealing with time-series and sequence modelling (Goodfellow et al., 2016, Chapter 10). Finally, a stability test of the control strategy will be conducted since the WWTP processes present unmodelled dynamics, uncertainties and non-linearities that compromise the controller's stability (Li and Zhu (2019)). In this case, classical stability tests cannot be performed since the proposed control strategy only relies on data obtained from the real process. Therefore, a stability test based on the estimation of the empirical transfer function of the signals involved in the control process is adopted (Rojas and Vilanova (2012)).

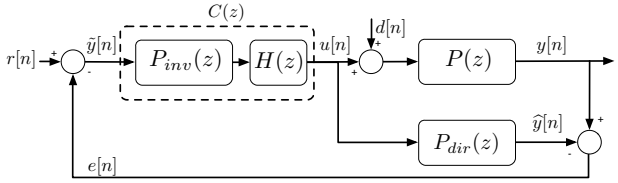

Fig. 2. IMC structure. $P_{dir}(z)$ and $P_{inv}(z)$ are the direct and inverse models or the process under control $P(z)$. $H(z)$ corresponds to a low-pass filter adopted to avoid bad behaviours at high frequencies.

3. LSTM-BASED IMC APPROACH

3.1 LSTM-based IMC

The proposed IMC has been implemented by adopting LSTM cells. The main point of these networks is that they implement a memory cell able to model sequences and time series. In terms of their memory cell, it considers a cell state which is propagated through time with the objective of storing the information of what has been previously observed. Besides, this cell state is updated accordingly to its input information. Therefore, the cell is able to manage its internal state determining if the input information is more relevant than the stored one or vice versa (Goodfellow et al., 2016, Chapter 10). Thus, in this work LSTMs are adopted to obtain the direct and inverse models of the process under control since the considered signals show a high correlation and time dependence. In such a context, the behaviour of the proposed IMC (see Fig. 2) is described as follows: The outputs of the process and its direct model correspond to

$$\begin{aligned} y[n] &= P(u[n] + d[n]) = S_{O,5}[n] \\ \widehat{y}[n] &= P_{dir}(u[n]) = \widehat{S}_{O,5}[n], \end{aligned} \tag{1}$$

where $u[n] = K_{La,5}[n]$ is the actuation variable and $d[n]$ are the weather perturbations entering in the real process. Here, $u[n]$ is computed by the IMC controller ($C(z)$) as

$$u[n] = C(\tilde{y}[n]) = H(P_{inv}(\tilde{y}[n])) = \widehat{K}_{La,5}[n], \tag{2}$$

where $P_{inv}(z)$ is the inverse of the process under control, $\tilde{y}[n]$ corresponds to the update of $r[n]$ with the mismatch between the real process and its direct model,

$$\tilde{y}[n] = r[n] - e[n] = r[n] - (y[n] - \widehat{y}[n]), \tag{3}$$

and $H(z)$ corresponds to a first order low-pass filter in charge of managing the controller's tolerance, i.e., the behaviour of $C(z)$ when unmodelled dynamics, inversion uncertainties, etc, are present in the system (Pisa et al. (2019a)). The filter cutt-off frequency ω_c (rad/s) is determined accordingly to the stability test applied to the IMC.

The main point here is that $P_{dir}(z)$ and $P_{inv}(z)$ are implemented adopting LSTM cells (see Fig. 3) to reduce the mismatch between the real process and the direct model as well as to avoid the loss of accuracy when the inverse model is computed (Kandasamy et al. (2018); Pisa et al. (2019a)). Thus, $P_{inv}(z)$ and $P_{dir}(z)$ are described as:

$$P_{inv}(z) = LSTM_{inv}(z) \qquad P_{dir}(z) = LSTM_{dir}(z). \tag{4}$$

Both architectures consider a total amount of 5 elements: the Sliding Window and the Normalisation layers, the LSTM cell itself with 100 hidden neurons per gate, the Linear activation function and the Denormalisation layer. They have a total amount of 5 inputs and one output signals which are determined accordingly to the purpose of the net: (i) $LSTM_{inv}$ considers the controlled variable ($S_{O,5}[n]$) as one of the inputs and the actuation variable ($\widehat{K}_{La,5}[n]$) as its output; (ii) $LSTM_{dir}$ considers the

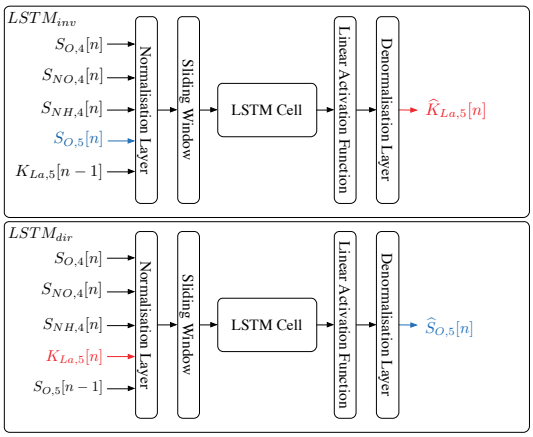

Fig. 3. $LSTM_{inv}$ and $LSTM_{dir}$ architectures. Actuation variable ($k_{La,5}$) is coloured in red whereas the controlled one ($S_{O,5}$) is coloured in blue.

$\widehat{K}_{La,5}[n]$ as one of the inputs and $\widehat{S}_{O,5}[n]$ as its output. Furthermore, each architecture also considers the last predicted value as another input. Besides, both architectures consider a common part of measurements to provide the net with more information about the processes being modelled. They correspond to the dissolved oxygen ($S_{O,4}$), the nitrate nitrogen ($S_{NO,4}$) and the ammonium ($S_{NH,4}$) at the fourth reactor tank. In terms of the layers, the Normalisation preprocessing one is in charge of normalising the input data towards zero-mean and unity variance with the objective of addressing data heterogeneity. Then, normalised data are sorted in time in the Sliding Window preprocessing layer. The length of this sliding window equals to 4 hours. Then, both LSTM cells predict the corresponding measurements which go through the Linear Activation Function to get the concentration prediction (Da Silva et al., 2017, Section 1.3). Finally, they are denormalised in the Denormalisation Layer.

Each architecture has a total of 42901 parameters that have been trained considering a whole year of BSM1 influent data sampled every 15 minutes (sampling frequency of 1.11 mHz) when different equally distributed dry, rainy and stormy weather episodes are considered. The LSTM hyperparameters (number of cells and hidden neurons) have been found performing a grid search: 200 training epochs with Adam optimiser and a learning rate equal to $1 \cdot 10^{-3}$ have been considered. Then, the LSTM models have been cross-validated adopting K-Fold method (5 folds) (Bergmeir et al. (2018)). After this, early stopping and L2 penalty equal to $1 \cdot 10^{-4}$ have been considered to mitigate overfitting problems (Goodfellow et al., 2016, Chapter 7).

3.2 IMC stability study

The robust stability of the IMC structure has to be computed in order to determine if the control approach can be considered or not. However, the classical stability analyses cannot be applied in our case since the proposed IMC is completely based on LSTMs and therefore, on data. For that reason, the stability of the proposed IMC approach will be computed based on the test explained in Rojas and Vilanova (2012). This test is mainly focused on the basis that neither mathematical models of the process under

control, nor for the inverse or direct models are available. Hence, it infers the transfer functions of the different IMC models by means of applying the Empirical Transfer Function Estimate (ETFE) (Ljung (1999)). ETFE considers that the frequency response of a system ($T(z)$), whose transfer function is unknown, can be inferred whenever pairs of input/output data ($u[n], y[n]$) are available. Therefore, its frequency response is computed as follows:

$$\widehat{T}(e^{j\omega}) = \frac{Y(e^{j\omega})}{U(e^{j\omega})}, \tag{5}$$

where $U(e^{j\omega})$ and $Y(e^{j\omega})$ are the Fourier transforms of input and output data, respectively. In such a context, the data-based stability test says that a system is stable if

$$|\widehat{P}_{dir}(e^{j\omega})\widehat{C}(e^{j\omega})l_m(\omega)| \leq 1, \tag{6}$$

where $\widehat{P}_{dir}(e^{j\omega})$ and $\widehat{C}(e^{j\omega})$ are the frequency response (inferred adopting (5)) of $P_{dir}(z)$ and $C(z)$, respectively. $1/|l_m(\omega)|$ is the multiplicative uncertainty bound which is defined as the stability limit of the system. Thus, if the product $|\widehat{P}(e^{j\omega})\widehat{C}(e^{j\omega})|$ is placed over $1/|l_m(\omega)|$ for a given frequency, it means that the stability of the system is not assured for this frequency (Rojas and Vilanova (2012)). In this case, $l_m(\omega)$ estimation is given by

$$l_m(\omega) = \frac{|P_{mismatch}(e^{j\omega})|}{|P_{dir}(e^{j\omega})|}, \tag{7}$$

where $|P_{mismatch}(e^{j\omega})|$ is the frequency response inferred from the mismatch $e[n]$ between the outputs of the process under control and the direct model when $u[n] = \widehat{K}_{La,5}[n]$ is considered as the input: $P_{mismatch}(e^{j\omega}) = E(e^{j\omega})/U(e^{j\omega})$.

The pairs of input/output data required to infer the different frequency responses are obtained considering an open-loop configuration, i.e., each pair of input/output data is obtained from each process when there is no interaction among them. Once the different frequency responses are inferred, the stability test is performed for each one. If the stability criterion shown in (6) is accomplished means that the IMC approach is stable. Otherwise, the robust stability of the system can be compromised for that frequency. Thus, after completing the test, those frequency ranges where the system is marginally stable will be determined.

4. RESULTS

Three tests have been conducted to determine the behaviour of the proposed IMC approach: (i) the Prediction performance test; (ii) the Stability test; and (iii) the IMC performance test. The first one is devoted to determining the prediction performance of the LSTM structures adopted to model the inverse and direct relationships between actuation and controlled variables of the process under control, i.e., $P_{inv}(z)$ and $P_{dir}(z)$. The metrics considered in this test are the determination coefficient (R^2), the Mean Absolute Error Percentage (MAPE), which is computed with denormalised data to avoid divisions by zero, and the Root Mean Squared Error (RMSE), which is measured in day^{-1} and mg/L in the cases of $P_{inv}(z)$ and $P_{dir}(z)$, respectively (Islam et al. (2012)). Results will be compared with the ones shown in Pisa et al. (2019a), where a similar approach considering MLP networks is proposed. The second test corresponds to the stability test of the IMC approach. It will determine which are those frequencies where the proposed approach is stable and therefore, if the IMC can be adopted or not depending on the frequency components of the signals involved in the control process. Finally, the last test is performed once the proposed IMC is implemented in BSM1 framework. It will determine the behaviour of the IMC approach when a closed-loop configuration is adopted. In this case, the considered metrics are the Integrated Absolute Error (IAE) and the Integrated Squared Error (ISE). Both are computed considering the BSM1 simulation protocol, i.e., those samples representing the WWTP behaviour between days 7 and 14 (Copp (2002)).

$$IAE = \sum_{n=day\,7}^{day\,14} |r[n]-y[n]| \qquad ISE = \sum_{n=day\,7}^{day\,14} (r[n]-y[n])^2. \tag{8}$$

4.1 Prediction performance

The prediction performance of the LSTM cells involved in the modelling of $P_{inv}(z)$ and $P_{dir}(z)$ has been contrasted with the MLP adopted in Pisa et al. (2019a) after their training process. Results in terms of the RMSE, MAPE and R^2 metrics are shown in Table. 1. As it is observed, the improvements of the LSTM modelling the direct relationships ($LSTM_{dir}$) w.r.t. the MLP one are around a 40% and a 77.42% in terms of RMSE and MAPE, respectively. In the case of $LSTM_{inv}$, its RMSE and MAPE improvements w.r.t MLP_{inv} are equal to a 45% and a 25.73%, respectively. Both LSTM cells are able to improve a 1.01% the MLPs' R^2 metric. Thus, these results show that LSTMs are the best option to implement the IMC since the input signals we are dealing with can be modelled as time-series.

4.2 Stability Test

Prediction performance has shown that LSTMs are the best option to implement the IMC approach. However, the stability of the LSTM cells and the whole structure has to be computed before determining the behaviour of the controller. As previously stated, the stability test requires pairs of input/output data to infer the frequency response of the different processes involved in the control. In the input/output data generation of the process under control and the direct model, hourly variations of the actuation signal $u[n] = K_{La,5}[n]$ between its minimum

Table 1. MLPs vs. LSTM prediction performance

Net	RMSE	MAPE[%]	R^2
MLP_{dir}	0.050	3.72	0.98
$LSTM_{dir}$	0.030	0.84	0.99
Improvement [%]	40	77.42	1.01
MLP_{inv}	0.082	5.48	0.98
$LSTM_{inv}$	0.045	4.07	0.99
Improvement [%]	45	25.73	1.01

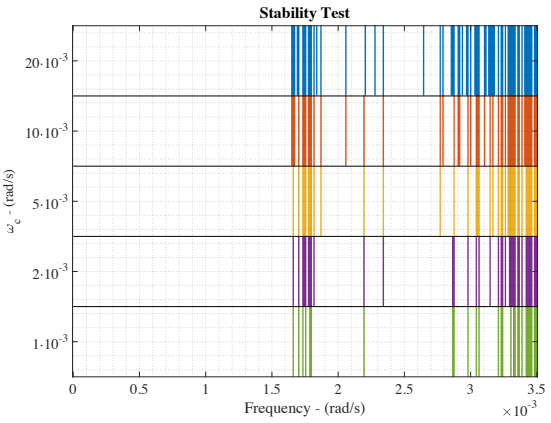

Fig. 4. Stability test performed to the IMC approach. Notice that this test has been performed for different configurations of $H(z)$ ω_c parameter.

and maximum values are considered. The rest of input values correspond to the default BSM1 influent data. The same pairs of input/output data will be used as the output/input data of the inverse model.

$l_m(\omega)$ is estimated to compute the multiplicative uncertainty of the system. This uncertainty corresponds to the bound determining the stability of the system since no frequency components over it are allowed (Rojas and Vilanova (2012)). Since $P_{dir}(e^{j\omega})$ and $C(e^{j\omega})$ are the inverse of each other, the product between the two frequency response should be 1 for all their components. However, there are some ranges where the product differs from 1 and is placed over the multiplicative uncertainty bound, which means that the stability of the IMC is not assured. If this is translated into the stability test, the frequencies where $|P_{dir}(e^{j\omega})\cdot C(e^{j\omega})|$ is placed above the multiplicative uncertainty bound are the ones where (6) is not accomplished. Here is where $H(z)$ makes sense because the lower the ω_c cutoff frequency, the lower the number of frequencies where the IMC stability is compromised (see Fig. 4).

Notwithstanding, the attenuation effect of the filter is also important: if ω_c is set to a very low frequency, the system stability will increase at the expense of degrading predictions and control performance. In this case, after analysing all the signals involved in the control process, we have observed that the highest frequency component, $\omega = 1.5 \cdot 10^{-3}$ rad/s, corresponds to $K_{La,5}(e^{j\omega})$ and $S_{O,5}(e^{j\omega})$ signals (see Fig. 5). Then, a cut-off frequency of $\omega_c = 10 \cdot 10^{-3}$ rad/s is considered in this work because ω_c is far enough of the input signals frequency components as well as the filter's attenuation effect is not appreciable until the $2 \cdot 10^{-3}$ rad/s (see Fig. 5). It is worth noting that although the performed analysis is valid for the BSM1 model, it can be still applied in a real environment as long as the BSM1 model is modified according to the real plant.

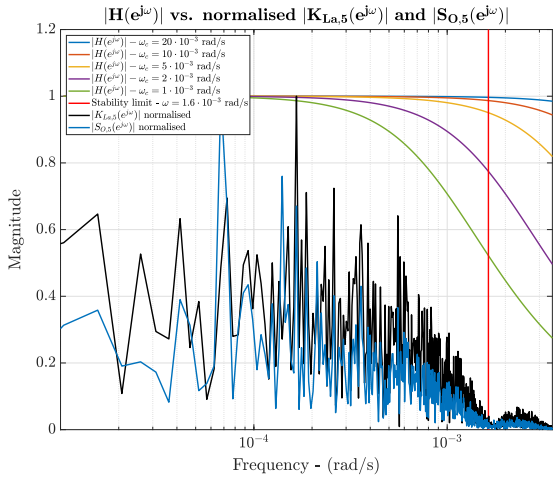

Fig. 5. $|H(e^{j\omega})|$ vs. $|K_{La,5}(e^{j\omega})|$ vs. $|S_{O,5}(e^{j\omega})|$.

4.3 IMC performance

Finally, the IMC approach has been implemented in BSM1 to track the $S_{O,5}$ concentrations. Weather perturbations have been considered, therefore, the IMC performance will show the suitability of this control approach in the set-point tracking tasks when dry, rainy and stormy weathers are present. Results are shown in Table 2, where the IAE and ISE metrics are shown. Two different $H(z)$ configurations of the IMC approach are considered: $\omega_{c,1} = 10 \cdot 10^{-3}$ rad/s and $\omega_{c,2} = 5 \cdot 10^{-3}$ rad/s. It is worth to notice that we have considered a variable $S_{O,5}$ set-point instead of a fix one at a value of 2 mg/L. Therefore, default PI results will differ from the ones provided in Alex et al. (2008). In that sense, the proposed IMC approach is able to improve the IAE and ISE metrics around a 24% and a 57% in average, respectively when $\omega_{c,1}$ equals to $10 \cdot 10^{-3}$ rad/s. In the case where $\omega_{c,2} = 5 \cdot 10^{-3}$ rad/s, the improvements are decreased 17 and 23 percentage points in average in terms of IAE and ISE. This means that the tracking process is better performed when the LSTM-based IMC approach is considered.

In terms of the $H(z)$ configurations, the IMC performance shows that $\omega_{c,1} = 10 \cdot 10^{-3}$ rad/s offers the best results while there is a worsening in the improvement when $\omega_{c,2} = 5 \cdot 10^{-3}$ rad/s is adopted. This is motivated by the aforementioned attenuation effect of the filter. For that reason, the configuration adopting $\omega_{c,1}$ has been considered: stability is still assured at the same time there is a significant improvement in the IMC control performance. The controlled ($S_{O,5}[n]$) and actuation ($K_{La,5}[n]$) signals generated in each case are shown in Fig. 6. Here, it is observed that both, $y[n]$ and $u[n]$ are exactly equal for all the considered weathers until rainy and stormy episodes start (at day 8 approximately (Qiao et al. (2018)). There, the generated $u[n]$ starts to fluctuate depending on the weather whereas the tracking process is performed well.

Table 2. Control performance

Default PI vs. IMC control strategies						
	Weathers					
	Dry		Rainy		Stormy	
Structure	IAE	ISE	IAE	ISE	IAE	ISE
PI	1.24	0.83	1.20	0.81	1.23	0.84
$IMC-\omega_{c,1}$	0.97	0.38	0.90	0.34	0.92	0.35
$IMC-\omega_{c,2}$	1.15	0.56	1.13	0.54	1.13	0.54
	Improvement [%] w.r.t. PI					
$IMC-\omega_{c,1}$	21.77	54.22	25.00	58.02	25.20	58.33
$IMC-\omega_{c,2}$	7.26	32.53	5.83	33.34	8.13	35.71

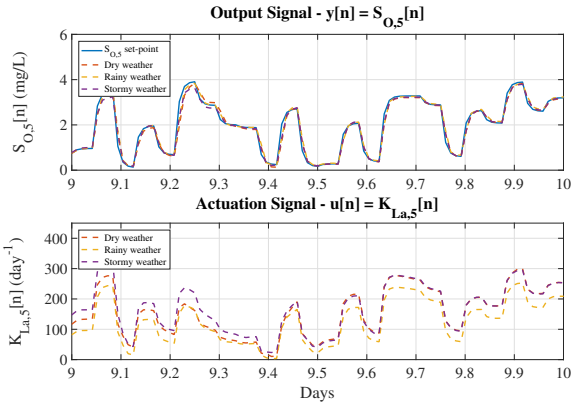

Fig. 6. IMC tracking process for different types of weather

5. CONCLUSION

The adoption of LSTM cells to implement an IMC approach has been discussed in this work. Here, the signals we are dealing with corresponds to WWTP concentrations which have the form of time-series with a strong time correlation between measurements. Moreover, the process to be controlled shows highly complex and non-linear dynamics. For that reason, LSTMs have been proposed to design the IMC strategy. Furthermore, one of the major contributions of this paper is placed in the data-based stability test performed to the IMC: The frequency response of control elements is inferred from input/output data since neither mathematical models nor transfer functions of the process under control have been computed.

In such a context, the proposed IMC approach has been tested in terms of prediction, stability and control performance to determine if it can be adopted in the $S_{O,5}$ control task. Results have shown that it improves between a 26% and a 77% the prediction performance offered by a similar approach adopting MLP networks. Besides, the stability test shows that this approach is marginally stable if signals considered in the control task show frequency components below $1.6 \cdot 10^{-3}$ rad/s. In this case, the highest frequency component corresponds to $1.5 \cdot 10^{-3}$ rad/s approximately. Therefore, the stability of the IMC is assured. Finally, the control performance shows that the IMC approach is able to improve the IAE and ISE metrics around a 24% and a 57% w.r.t. the BSM1 default control.

REFERENCES

Alex, J. et al. (2008). Benchmark simulation model no. 1 (BSM1). *Report by the IWA Taskgroup on Benchmarking of Control Strategies for WWTPs.*

Bergmeir, C., Hyndman, R.J., and Koo, B. (2018). A note on the validity of cross-validation for evaluating autoregressive time series prediction. *Computational Statistics & Data Analysis*, 120.

Copp, J.B. (2002). *The COST Simulation Benchmark: Description and Simulator Manual: a Product of COST Action 624 and COST Action 682.* EUR-OP.

Da Silva, I.N., Spatti, D.H., Flauzino, R.A., Liboni, L.H.B., and dos Reis Alves, S.F. (2017). Artificial neural networks. *Cham: Springer International Publishing.*

Directive, EUW (1991). Council Directive 91/271/EEC of 21 May 1991 concerning urban waste water treatment (91/271/EEC). *J. Eur. Commun*, 34, 40.

Goodfellow, I., Bengio, Y., and Courville, A. (2016). *Deep learning.* MIT press.

Henze, M., Grady Jr, L., Gujer, W., V. R Marais, G., and Matsuo, T. (1987). Activated Sludge Model No 1. *IAWPRC Scientific and technical Reports*, 29.

Islam, S., Keung, J., Lee, K., and Liu, A. (2012). Empirical prediction models for adaptive resource provisioning in the cloud. *Future Generation Computer Systems*, 28(1), 155–162.

Kandasamy, N.K., Karunagaran, G., Spanos, C., Tseng, K.J., and Soong, B.H. (2018). Smart lighting system using ANN-IMC for personalized lighting control and daylight harvesting. *Building and Environment*, 139, 170–180.

Li, P. and Zhu, G. (2019). Robust internal model control of servo motor based on sliding mode control approach. *ISA Transactions.*

Ljung, L. (1999). *System Identification, Theory for the User.* Pretince Hall, 2nd edition.

Nadiri, A.A., Shokri, S., Tsai, F.T.C., and Moghaddam, A.A. (2018). Prediction of effluent quality parameters of a wastewater treatment plant using a supervised committee fuzzy logic model. *Journal of cleaner production*, 180, 539–549.

Pisa, I., Morell, A., Vicario, J.L., and Vilanova, R. (2019a). ANN-based Internal Model Control strategy applied in the WWTP industry. In *24th IEEE International Conference on Emerging Technologies and Factory Automation (ETFA).*

Pisa, I., Santín, I., Morell, A., Vicario, J.L., and Vilanova, R. (2019b). LSTM based Wastewater Treatment Plants operation strategies for effluent quality improvement. *IEEE Access*, 7(1), 159773–159786.

Qiao, J.F., Hou, Y., Zhang, L., and Han, H.G. (2018). Adaptive fuzzy neural network control of wastewater treatment process with multiobjective operation. *Neurocomputing*, 275, 383–393.

Rojas, J. and Vilanova, R. (2012). Data-driven based IMC control. *International Journal of Innovative Computing, Information and Control*, 8(3), 1557–1574.

Sadeghassadi, M., Macnab, C.J., Gopaluni, B., and Westwick, D. (2018). Application of neural networks for optimal-setpoint design and MPC control in biological wastewater treatment. *Computers and Chemical Engineering*, 115, 150–160.

Sarvari, P.A., Ustundag, A., Cevikcan, E., Kaya, I., and Cebi, S. (2018). Technology Roadmap for Industry 4.0. In *Industry 4.0: Managing The Digital Transformation.* Springer.

Shen, W., Chen, X., and Corriou, J.P. (2008). Application of model predictive control to the BSM1 benchmark of wastewater treatment process. *Computers and Chemical Engineering*, 32(12), 2849–2856.

Vilanova, R., Santin, I., Pedret, C., and Barbu, M. (2018). Event-based control for dissolved oxygen and nitrogen in wastewater treatment plants. In *2018 22nd International Conference on System Theory, Control and Computing (ICSTCC)*, 212–217. IEEE.